

Experimental Investigation of Nonideal Two-qubit Quantum-state Filter by Quantum Process Tomography

Yoshihiro Nambu and Kazuo Nakamura

*Fundamental and Environmental Research Laboratories,
NEC, 34 Miyukigaoka, Tsukuba, Ibaraki 305-8501, Japan*

We used quantum process tomography to investigate and identify the function of a nonideal two-qubit quantum-state filters subject to various degree of decoherence. We present a simple decoherence model that explains the experimental results and point out that a beamsplitter followed by a post-selection process is not, as commonly believed, a singlet-state filter. In the ideal case it is a triplet-state filter.

PACS numbers: 03.65.Wj, 42.50.Dv

Characterization of quantum devices is important, and the characterization of single- and two-qubit devices is particularly important because a single-qubit rotation gate and a two-qubit controlled-NOT (C-NOT) gate are two building blocks of the quantum computer[1]. The quantum systems in actual devices may undergo nonunitary state evolution because they interact with their environments, so identifying and understanding the function of such nonideal devices are of practical importance. Nonideal devices can be characterized by quantum process tomography (QPT)[2, 3, 4], and this method has been used to characterize single-qubit transmission channels[5, 6] and rotation gates for photons[7], gates for ensembles of two-qubit systems in NMR[8], and a two-qubit quantum-state filter[9] and a C-NOT gate for photons[10].

This letter reports the QPT of a quantum-state filter—the beamsplitter (BS) in a Hong-Ou-Mandel (HOM) interferometer[11, 12]—as a demonstration how the function of two-qubit devices can be identified experimentally. The result of an earlier investigation of the nearly ideal filter[9] was inconsistent with a common belief that an ideal BS followed by a post-selection process—only the outcomes where the two input photons come out in two output ports are taken into account—behaves as a singlet-state filter [12, 13], but the reason for this inconsistency was not fully understood. To resolve this problem, we have investigated the function of the nonideal filters subject to various degree of decoherence and have identified two leading contributions to the operator-sum representation of the quantum operation for them[1, 2, 14]. Here we present a model that explains our experimental results and resolve the above inconsistency.

Let us start by introducing the process matrix[10], which offers us the most general description of the quantum device allowed in quantum mechanics, and showing how to obtain it experimentally. Consider a two-qubit device whose function is to map a two-qubit input density operator $\hat{\rho}_{in}$ to a two-qubit output density operator $\hat{\rho}_{out} = \mathcal{E}(\hat{\rho}_{in})$, where \mathcal{E} is a completely positive linear map[14]. The map \mathcal{E} is considered a superoperator acting on positive operators[15]. Let us introduce the set of

standard operator basis $\{\hat{X}_k\}_{k=0}^3$ that spans two-qubit operator space[16], where $\hat{X}_{\langle ij \rangle} = |i\rangle\langle j|$ ($i, j = 0, 1$) and $\langle ij \rangle := 2i + j$. Then \mathcal{E} can be expanded as

$$\mathcal{E}(\hat{\rho}) = \sum_{k,l,m,n=0}^3 (\chi^S)_{[kl][mn]} \hat{X}_k \otimes \hat{X}_l \hat{\rho} \hat{X}_m^\dagger \otimes \hat{X}_n^\dagger, \quad (1)$$

where $[kl] := 4k + l$ [15]. A 16×16 positive Hermitian matrix χ^S fully characterizes the function of quantum device and is called the process matrix in the standard operator basis[10].

We can transform χ^S into the process matrix in any operator basis set $\{\hat{A}_\alpha\}_{\alpha=0}^{15}$ that spans the two-qubit operator space. Note that \hat{A}_α may be defined either locally or nonlocally. For example, the Kronecker products of the Pauli operator basis $\hat{B}_{[kl]} = \hat{E}_k \otimes \hat{E}_l$ ($k, l = 0, \dots, 3$), where $\{\hat{E}_k\} = \{\hat{\sigma}_0/\sqrt{2}, \hat{\sigma}_1/\sqrt{2}, \hat{\sigma}_2/\sqrt{2}, \hat{\sigma}_3/\sqrt{2}\}$ and $\hat{\sigma}_0$ denotes an identity operator, is a local operator basis, whereas the outer product $\hat{C}_{[kl]} = |\Phi_k\rangle\langle\Phi_l|$, where $|\Phi_k\rangle$ are Bell states, is a nonlocal one. The operator basis \hat{A}_α is, in general, unitarily related to the standard operator basis $\hat{X}_k \otimes \hat{X}_l$. That is, $\hat{A}_\alpha = \sum_{k,l=0}^3 (U)_{[kl]\alpha} \hat{X}_k \otimes \hat{X}_l$, where U is a 16×16 unitary matrix. Then \mathcal{E} can be expanded using \hat{A}_α as follows:

$$\mathcal{E}(\hat{\rho}) = \sum_{\alpha,\beta=0}^{15} (\chi^A)_{\alpha\beta} \hat{A}_\alpha \hat{\rho} \hat{A}_\beta^\dagger, \quad (2)$$

where $\chi^A = U^\dagger \chi^S U$. Therefore, χ^A is given by the unitary transform of χ^S .

To obtain χ^S , it is sufficient to determine the associated four-qubit state[17]. Let us consider a four-qubit system composed of the two two-qubit systems 1-2 and 3-4 and introduce the double-ket notation $|I\rangle\rangle := (\hat{I} \otimes \hat{I})|\Phi\rangle$ to denote the bipartite state, where $|\Phi\rangle = \sum_{i=0}^1 |i, i\rangle$ is the unnormalized maximally entangled state[4, 16]. Let us introduce the unnormalized four-qubit density operator $\hat{\mathcal{D}}_{\mathcal{E}}$ associated with \mathcal{E} by $\hat{\mathcal{D}}_{\mathcal{E}} = \mathcal{E}^{(13)} \otimes \mathcal{I}^{(24)}(|I\rangle\rangle_{12}\langle\langle I| \otimes |I\rangle\rangle_{34}\langle\langle I|)$, where \mathcal{I} is an identity map and the superscript and subscript respectively denote the space on which each map acts and

the space to which the operator belongs[17]. Using Eq. 1 and $|X_k\rangle\rangle := (\hat{X}_k \otimes \hat{I})|\Phi\rangle$, we can rewrite $\hat{\mathcal{D}}_{\mathcal{E}}$ as

$$\hat{\mathcal{D}}_{\mathcal{E}} = \sum_{k,l,m,n=0}^3 (\chi^S)_{[kl][mn]} |X_k\rangle\rangle |X_l\rangle\rangle \langle\langle X_m| \langle\langle X_n|. \quad (3)$$

If we note that $|X_{\langle ij \rangle}\rangle\rangle \equiv |i, j\rangle$, Eq. 3 indicates that χ^S agrees exactly with the density matrix of the associated state $\hat{\mathcal{D}}_{\mathcal{E}}$ given in the standard state basis. Evaluation of the process matrix is thus reduced to evaluation of the associated state $\hat{\mathcal{D}}_{\mathcal{E}}$.

To obtain $\hat{\mathcal{D}}_{\mathcal{E}}$, it is sufficient to evaluate all the maps $\mathcal{E}(\hat{X}_{\langle ij \rangle} \otimes \hat{X}_{\langle kl \rangle})$ for all the elements of the standard operator basis $\hat{X}_{\langle ij \rangle} \otimes \hat{X}_{\langle kl \rangle}$, since we can obtain the permutation equivalent of $\hat{\mathcal{D}}_{\mathcal{E}}$ —that is, $\tilde{\mathcal{D}}_{\mathcal{E}} = \hat{P}_{23}\hat{P}_{12}\hat{P}_{34}\hat{\mathcal{D}}_{\mathcal{E}}\hat{P}_{34}\hat{P}_{12}\hat{P}_{23} = \mathcal{I}^{(12)} \otimes \mathcal{E}^{(34)}(|I\rangle\rangle_{13}\langle\langle I| \otimes |I\rangle\rangle_{24}\langle\langle I|)$ —by using the following identity:

$$\tilde{\mathcal{D}}_{\mathcal{E}} \equiv \sum_{k,l=0}^3 \hat{X}_k \otimes \hat{X}_l \otimes \mathcal{E}(\hat{X}_k \otimes \hat{X}_l), \quad (4)$$

where \hat{P}_{ij} is a permutation operator between the systems i and j . To evaluate these maps, we need only to use state tomography[18] to evaluate the 16 two-qubit output states $\{\mathcal{E}(\hat{\rho}_i^{(1)} \otimes \hat{\rho}_j^{(2)})\}_{i,j=0}^3$ associated with the set of 16 separable input states, where $\hat{\rho}_i \in \{|0\rangle\langle 0|, |1\rangle\langle 1|, |+\rangle\langle +|, |\circlearrowleft\rangle\langle \circlearrowleft|\}$, $|+\rangle = 1/\sqrt{2}(|0\rangle + |1\rangle)$, and $|\circlearrowleft\rangle = 1/\sqrt{2}(|0\rangle + i|1\rangle)$ [2, 3, 4]. We therefore can obtain the process matrix directly from the experimental data without using a matrix inversion procedure[1, 2].

We used the above procedure to obtain the process matrices for nonideal two-qubit quantum-state filters. The experimental setup is shown in Fig. 1. A 0.3-mm-thick type-I crystal (BBO) was pumped by frequency-tripled pulses generated by 100-fs pulses from a mode-locked Ti:sapphire laser (repetition rate ≈ 82 MHz). Pairs of horizontally polarized 532-nm photons were generated and those traveling in two directions 90° from the pump beam were selected by 5-mm irises (1 m from the crystal) and identical 3-nm-width filters (IF) placed before the detectors. They were injected into a HOM interferometer[9, 11, 12] having a broadband non-polarizing cube BS (Suruga Seiki model S322-20-550). The horizontally (H) and vertically (V) polarized states (respectively $|0\rangle$ and $|1\rangle$) and the other two states required for the QPT were prepared by half- and quarter-wave plates (HWP and QWP) placed immediately before the BS. Down-converted photons were incident on the BS at 45° . After the BS, polarization analyzers consisting of a QWP and a HWP followed by a Glan-Thompson prism (POL) and a single-photon counting module (PMT) performed projective measurements onto the set of the 16 product states $\{\hat{\rho}_i^{(1)} \otimes \hat{\rho}_j^{(2)}\}_{i,j=0}^3$. Only signals coincident at the two PMTs were recorded, and the associated 16 output states $\{\mathcal{E}(\hat{\rho}_i^{(1)} \otimes \hat{\rho}_j^{(2)})\}_{i,j=0}^3$ were evaluated by state tomography[18]. Note that we used unnormalized out-

put density matrices because the state filtering is trace-decreasing process whose output intensity depends on the input state.

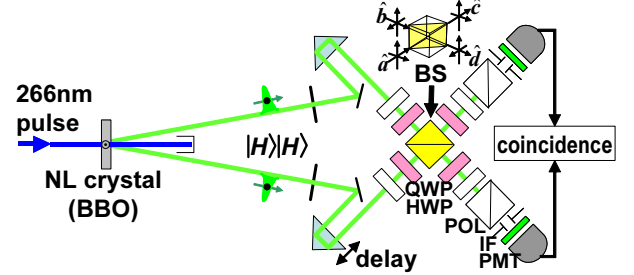


FIG. 1: Experimental setup to investigate the beamsplitter.

We used optical trombones to equalize the two path lengths to within the coherence length l_c of the down-converted photons ($\approx 200 \mu m$). Two two-photon amplitudes contributing to coincidence detection—*i.e.*, that both photons are reflected ($r-r$) or that both are transmitted ($t-t$)—were initially ($\tau = 0$) aligned to overlap both spatially and temporally, giving a HOM dip visibility of 85% as shown in Fig. 2. In this case, the BS is commonly thought to work as a singlet-state filter[12, 13]. To investigate the nonideal filter, we introduced a delay τ in one arm by moving one of the trombone prisms. The larger the τ is, the smaller the overlap of the two amplitudes is and the more the temporal and polarization information of the photon pair is entangled. We will show later that this results in decoherence if we observe only the polarization information.

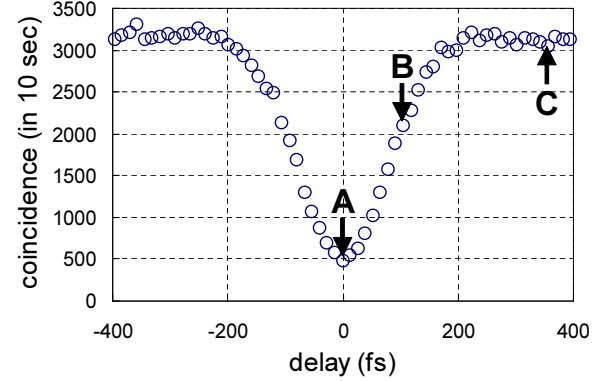


FIG. 2: HOM dip observed in the coincidence record. Arrows indicate delays τ of (A) 0, (B) 100, and (C) 350 fs introduced in one of the two arms.

We obtained the process matrices χ^F associated with three-delay conditions ($\tau = 0, 100$, and 350 fs). To make the results clear, we represent them here in the nonlocal operator basis $\hat{F}_{[ij]} = (\hat{E}_i \otimes \hat{E}_j)\hat{U}_S$, where \hat{U}_S is a swap operator. They are shown in Fig. 3, where space is saved by showing only the real parts. What is most interest-

ing is that the contribution of $(\chi^F)_{15\ 15}$ increases with increasing delay τ .

This result is consistent not with the common belief but with what was pointed out by Mitchell *et al.*[9]. Indeed, we found that our results are well reproduced if we assume that $\mathcal{E}(\hat{\rho})$ has an operator-sum representation with two Kraus operators $\hat{\mathcal{P}}^-$ and $\hat{\mathcal{P}}^+$ [1, 14]:

$$\mathcal{E}(\hat{\rho}) = (1-p)\hat{\mathcal{P}}^-\hat{\rho}\hat{\mathcal{P}}^{-\dagger} + p\hat{\mathcal{P}}^+\hat{\rho}\hat{\mathcal{P}}^{+\dagger}, \quad (5)$$

$$\hat{\mathcal{P}}^\pm = \mathcal{T}\hat{U}_I \pm \mathcal{R}\hat{U}_3(\theta_1, \theta_2)\hat{U}_S, \quad (6)$$

where p ($0 \leq p \leq 1/2$) is a parameter that can be interpreted as the degree of decoherence and where $\hat{U}_3(\theta_1, \theta_2) = e^{i\theta_1\hat{\sigma}_3/2}\hat{\sigma}_3 \otimes e^{-i\theta_2\hat{\sigma}_3/2}\hat{\sigma}_3$, which explains the large contribution of $(\chi^F)_{15\ 15}$ instead of $(\chi^F)_{00\ 00}$ as would be expected for the nonideal singlet-state filter. The Kraus operators $\hat{\mathcal{P}}^-$ and $\hat{\mathcal{P}}^+$ correspond respectively to the operator for the ideal state-filter and the noise operator. Note that Kraus operators are not unique and are not necessarily orthogonal[1]. Figure 4 shows the process matrices calculated using the measured value $\mathcal{R}/\mathcal{T} = 0.76$ and appropriate values of the parameters θ_1 , θ_2 , and p . As shown in Fig. 4, Eqs. 5 and 6 well reproduced the experimental results. It follows that the operator $\hat{\mathcal{P}}^-$ describing ideal operation deviates from the singlet-state because of the factor $\hat{U}_3(\theta_1, \theta_2)$, which is consistent with Ref. [9].

To understand these results, we need a decoherence model. Let us first call our attention to the function of the BS in the polarization space. Let \hat{a} and \hat{b} (\hat{c} and \hat{d}) denote input (output) field operators of the BS, and the polarization be indicated by subscripts (*e.g.*, by \hat{a}_H and \hat{a}_V for the H - and V -polarized field operators). If we use a right-handed coordinate system defined by the positive directions of H -, V - polarized field (p and s components) and propagation vector (Fig. 1) to describe the input and output fields, their operator equations are given by:

$$\begin{aligned} \hat{c}_H &= \sqrt{\mathcal{T}}\hat{a}_H + ie^{i(\Gamma+\pi)}\sqrt{\mathcal{R}}\hat{b}_H, \\ \hat{d}_H &= ie^{-i(\Gamma+\pi)}\sqrt{\mathcal{R}}\hat{a}_H + \sqrt{\mathcal{T}}\hat{b}_H, \\ \hat{c}_V &= \sqrt{\mathcal{T}}\hat{a}_V + ie^{i\Delta}\sqrt{\mathcal{R}}\hat{b}_V, \\ \hat{d}_V &= ie^{-i\Delta}\sqrt{\mathcal{R}}\hat{a}_V + \sqrt{\mathcal{T}}\hat{b}_V, \end{aligned} \quad (7)$$

where \mathcal{T} and \mathcal{R} are respectively the transmission and reflection coefficients of the BS. We have assumed that the p and s components of the field respectively acquire phase shifts $\Gamma + \pi$ and Δ upon reflection. The factor π accounts for abrupt change in p - s phase shift due to nonadiabatic changes in the \mathbf{k} vector upon reflection, which has been frequently noted in the papers concerning the topological phase effect in optics [20, 21, 22]. Note that the helicity of a photon in a state $|\circlearrowleft\rangle$ changes sign upon reflection from the BS but not upon transmission through the BS if $\Delta - \Gamma = 0$. If we consider the output fields that can contribute to coincidence measurement, we conclude from Eqs. 7 that the BS projects the input state onto $\hat{\mathcal{P}}^-$ with $\theta_1 = \theta_2 = \Delta - \Gamma$, which may be finite for a non-polarizing BS. Note that the projector $\hat{\mathcal{P}}^-$ is the coherent

sum of the identity operator \hat{U}_I associated with transmission and the operator $\hat{U}_3(\theta_1, \theta_2)\hat{U}_S$ associated with reflection, where $\hat{U}_3(\theta_1, \theta_2)$ accounts for the helicity reversal and the extra p - s phase shift upon reflection.

Although the above description may suffice when $\tau = 0$, the temporal (T) space of the two-photon state should be taken into account when $\tau \neq 0$. Concerning the temporal state space, it would be reasonable to assume that the BS leaves the state untouched on transmission and swaps the state on reflection. We thus assume that the function of the BS is described by the following operator entangled with respect to the polarization and temporal state spaces:

$$\hat{\mathcal{P}}^{PT} = \mathcal{T}\hat{U}_I^P \otimes \hat{U}_I^T - \mathcal{R}\hat{U}_3^P(\theta_1, \theta_2)\hat{U}_S^P \otimes \hat{U}_S^T, \quad (8)$$

where the superscripts indicate the space on which each operator acts. We further assume that input state is unentangled, *i.e.*, that it is a product state of polarization state $\hat{\rho}$ and temporal state $\hat{\omega}$. Then, by partially tracing over the temporal degree of freedom, we obtain the following output polarization state $\mathcal{E}(\hat{\rho})$ consistent with Eqs. 5 and 6:

$$\begin{aligned} \mathcal{E}(\hat{\rho}) &= \text{Tr}_T \hat{\mathcal{P}}^{PT} (\hat{\rho} \otimes \hat{\omega}) \left(\hat{\mathcal{P}}^{PT} \right)^\dagger \\ &= (1-p)\hat{\mathcal{P}}^-\hat{\rho}\hat{\mathcal{P}}^{-\dagger} + p\hat{\mathcal{P}}^+\hat{\rho}\hat{\mathcal{P}}^{+\dagger}, \end{aligned} \quad (9)$$

where the parameter p depends on the overlap of the two-photon amplitudes contributing to coincidence detection (r - r or t - t) and thus on the delay τ . Ideally, p is zero if $\tau = 0$, increases as τ increases, and approaches $1/2$ when $\tau \rightarrow \infty$. Figure 4 shows that this model largely explains the experimental results, except that θ_1 is not actually equal to θ_2 as in the model. The reason is uncertain, but this inequality may be due to polarization-dependent \mathcal{R}/\mathcal{T} ignored in the model.

We conclude that the function of the ideal BS is described by $\hat{\mathcal{P}}^-$, which depends on the p - s phase shift as well as the coefficients \mathcal{R} and \mathcal{T} . These parameters obviously depend on the detailed design of the BS. Properly designed BS would satisfy $\mathcal{R}/\mathcal{T} = 1$ and $\Delta - \Gamma = 0$ simultaneously, at least for photons that have a particular wavelength and are incident at 45° . In this idealized case, $\hat{\mathcal{P}}^-$ agrees with one of the four Bell states: a triplet state. This shows that the common belief that an ideal BS behaves as a singlet-state filter is a misconception due to overlooking the helicity reversal of the photon upon reflection at the BS.

In summary, we used QPT to investigate the nonideal two-qubit quantum-state filter and identify its function. We showed that our results are satisfactorily explained by a simple model with several reasonable assumptions that a common belief about the function of a BS followed by post-selection process is mistaken.

We thank S. Ishizaka and A. Tomita for their helpful discussions. This work was supported by the CREST program of the Japan Science and Technology Agency.

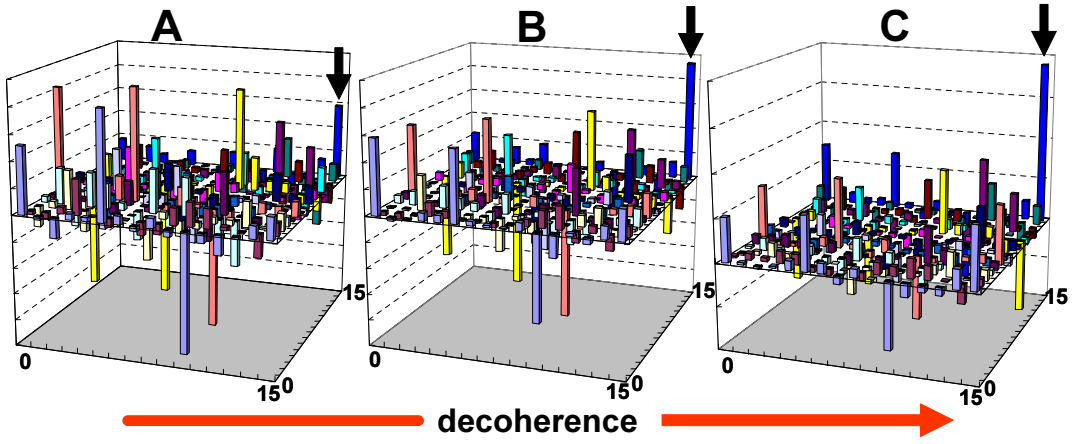


FIG. 3: The process matrices of the state filter obtained for delays τ of (A) 0, (B) 100, and (C) 350 fs. Only the real parts of the matrices are shown (in arbitrary units). Vertical arrows indicate the diagonal elements $(\chi^F)_{15,15}$.

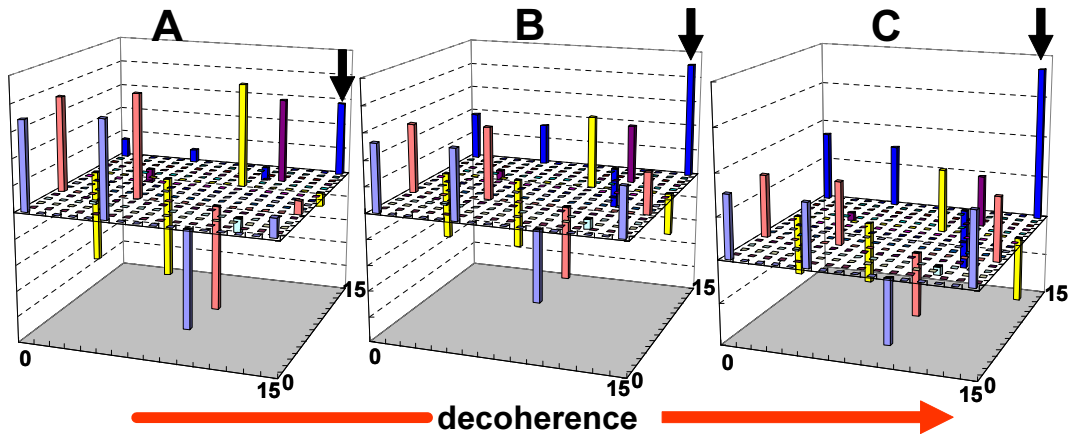


FIG. 4: Calculated process matrices corresponding to Fig. 3 (see text). The following parameters were used: (A) $p = 0.14$, (B) $p = 0.325$, (C) $p = 0.5$ and the common parameters $\mathcal{R}/\mathcal{T} = 0.76$, $\theta_1 \approx 0.41\pi$, and $\theta_2 \approx 0.076\pi$.

[1] I. L. Chuang and M. A. Nielsen, *Quantum Information and Quantum Computation* (Cambridge University Press, Cambridge, 2000).

[2] I. L. Chuang and M. A. Nielsen, *J. Mod. Opt.* **44**, 2455 (1997).

[3] J. F. Poyatos *et al.*, *Phys. Rev. Lett.* **78**, 390 (1997).

[4] G. M. D'Ariano and P. Lo Presti, *Phys. Rev. Lett.* **86**, 4195 (2001); *Phys. Rev. Lett.* **91**, 047902 (2003).

[5] Y. Nambu *et al.*, *Proc. SPIE Int. Soc. Opt. Eng.* **4917**, 13 (2002).

[6] J. B. Altepeter *et al.*, *Phys. Rev. Lett.* **90**, 193601 (2003).

[7] F. De Martini *et al.*, *Phys. Rev. A* **67**, 62307 (2003).

[8] A. M. Childs *et al.* *Phys. Rev. A* **64**, 12314 (2001).

[9] M. W. Mitchell *et al.*, *Phys. Rev. Lett.* **91**, 120402 (2003).

[10] J. L. O'Brien *et al.*, *quant-ph/0402166*.

[11] C. K. Hong *et al.*, *Phys. Rev. Lett.* **59**, 2044 (1987).

[12] K. Mattle *et al.*, *Phys. Rev. Lett.* **76**, 4656 (1996).

[13] S. L. Braunstein and A. Mann, *Phys. Rev. A* **51**, R1727 (1995).

[14] K. Kraus, *State, Effects, and Operations*, Lecture Notes in Physics Vol. 190 (Springer, Berlin, 1983).

[15] P. Rungta *et al.*, *quant-ph/0001075*; P. Rungta *et al.*, *quant-ph/0102040*.

[16] G. M. D'Ariano *et al.*, *Phys. Lett. A* **272**, 32 (2000).

[17] J. I. Cirac *et al.*, *Phys. Rev. Lett.* **86**, 544 (2001); W. Dür *et al.*, *Phys. Rev. A* **64**, 12317 (2001).

[18] Y. Nambu *et al.*, *Phys. Rev. A* **66**, 33816 (2002).

[19] J. M. Bennett, in *Handbook of Optics*, edited by M. Bass (McGraw-Hill, New York, 1995), Chap. 5.

[20] M. Kitano *et al.*, *Phys. Rev. Lett.* **58**, 523 (1987).

[21] M. V. Berry, *Nature (London)* **326**, 277 (1987).

[22] R. Y. Chiao *et al.*, *Phys. Rev. Lett.* **60**, 1214 (1988).